

Star Formation Efficiency at Intermediate Redshift

F. Combes¹, S. García-Burillo², J. Braine³, E. Schinnerer⁴,
F. Walter⁴, L. Colina⁵

¹Observatoire de Paris, LERMA (CNRS:UMR8112),
61 Av. de l'Observatoire, F-75014, Paris, France
email: francoise.combes@obspm.fr

²Observatorio Astronómico Nacional (OAN)-Observatorio de Madrid,
Alfonso XII, 3, 28014-Madrid, Spain

³Laboratoire d'Astrophysique de Bordeaux, UMR 5804, Université Bordeaux I,
BP 89, 33270 Floirac, France

⁴Max-Planck-Institut für Astronomie (MPIA), Königstuhl 17, 69117 Heidelberg, Germany

⁵Departamento de Astrofísica, Centro de Astrobiología (CSIC/INTA),
Torrejón de Ardoz, 28850 Madrid, Spain

Abstract. Star formation is evolving very fast in the second half of the Universe, and it is as yet unclear whether this is due to evolving gas content, or evolving star formation efficiency (SFE). We have carried out a survey of ultra-luminous galaxies (ULIRG) between $z=0.2$ and 1, to check the gas fraction in this domain of redshift which is still poorly known. Our survey with the IRAM-30m detected 33 galaxies out of 69, and we derive a significant evolution of both the gas fraction and SFE of ULIRGs over the whole period, and in particular a turning point around $z=0.35$. The result is sensitive to the CO-to-H₂ conversion factor adopted, and both gas fraction and SFE have comparable evolution, when we adopt the low starburst conversion factor of $\alpha = 0.8 \text{ M}_{\odot} (\text{K km s}^{-1} \text{ pc}^2)^{-1}$. Adopting a higher α will increase the role of the gas fraction. Using $\alpha = 0.8$, the SFE and the gas fraction for $z\sim 0.2-1.0$ ULIRGs are found to be significantly higher, by a factor 3, than for local ULIRGs, and are comparable to high redshift ones. We compare this evolution to the expected cosmic H₂ abundance and the cosmic star formation history.

Keywords. galaxies: evolution — galaxies: ISM — galaxies: interactions — galaxies: starburst — radio lines: galaxies

1. Introduction

Star formation (SF) was proceeding at a much faster rate in galaxies in the first half of the universe's history, and the most striking feature in the cosmic SF rate density is the decline by a factor ~ 10 since $z=1$ (Madau *et al.* 1998, Hopkins & Beacom 2006). Several factors could be invoked to explain such a behavior: first the gas fraction in star forming galaxies is likely to have been higher in the past, as already suggested by CO surveys, tracing the molecular gas content of galaxies. Locally, the gas fraction for giant spirals is about 7-10% (Leroy *et al.* 2008, Saintonge *et al.* 2011a), while at $z\sim 1.2$ it increases to $34\pm 5\%$ and at $z\sim 2.3$ to $44\pm 6\%$ (Tacconi *et al.* 2010, Daddi *et al.* 2010). Second, the star formation efficiency might have been higher in the past, due to the dynamical trigger of galaxy interactions, whose frequency increases with redshift (e.g. Conselice *et al.* 2009, Kartaltepe *et al.* 2010), and also the more violent instabilities in more unstable disks, with lower bulge-to-disk ratios. The star formation efficiency (SFE) defined as the ratio of SFR to gas content, has been observed to increase with redshift (e.g. Greve *et al.* 2005), even for

the most extreme starbursts, represented by ultra-luminous infrared galaxies (ULIRG). This tendency is however supported mainly by comparing local and high- z galaxies, at $z > 1$, and very little is known about the molecular gas content of galaxies at intermediate redshift between $z = 0.2$ and 1. This CO desert is mainly due to observational difficulties, and motivated our CO survey of starburst galaxies in this redshift range. A first study at $0.2 < z < 0.6$ (Combes *et al.* 2011) has indeed confirmed a strong increase of SFE in this redshift range.

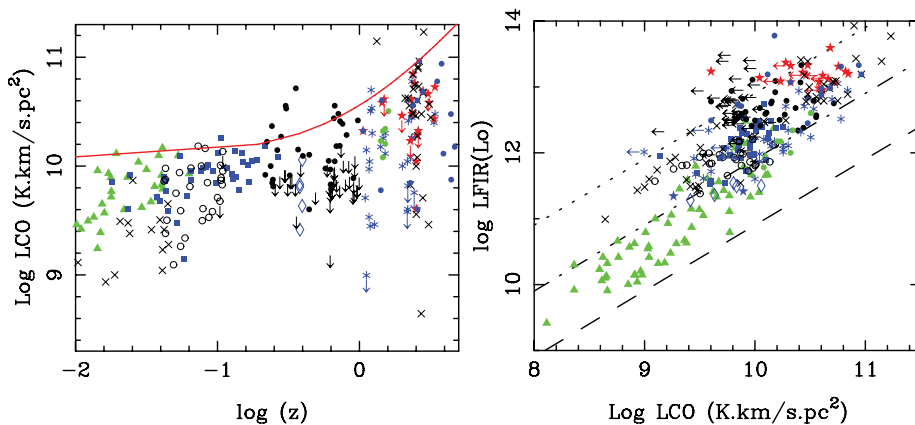


Figure 1. Left: CO luminosities, a proxy for total H_2 masses, versus redshift, for the objects of our sample (filled black circles, and arrows as upper limits), compared to various data from the literature: green triangles are from Gao & Solomon (2004), blue squares from Solomon *et al.* (1997), open circles from Chung *et al.* (2009), blue diamonds from Geach *et al.* (2009, 2011), black crosses from Iono *et al.* (2009), red stars, from Greve *et al.* (2005), green filled circles from Daddi *et al.* (2010), blue asterisks from Genzel *et al.* (2010), and blue filled circles from Solomon & vanden Bout (2005). For illustration purposes only, the red curve is the power law in $(1+z)^{1.6}$ for Ω_{H_2}/Ω_{HI} proposed by Obreschkow & Rawlings (2009). **Right:** Correlation between far infrared and CO luminosities for the same data. The 3 lines are for $L_{FIR}/M(H_2) = 10, 100$ and $1000 L_{\odot}/M_{\odot}$ from bottom to top, assuming a conversion factor $\alpha = 0.8 M_{\odot} (K km s^{-1} pc^2)^{-1}$. The three lines correspond to gas depletion time-scales of 580 (bottom), 58 (middle) and 5.8 Myr (top).

2. Star formation efficiency and gas fraction

We have now completed our CO survey of 69 starburst galaxies with $0.2 < z < 1.0$, and obtained a global detection rate of 48%. Since the conversion factor is a key parameter in this study, we have obtained CO detections in several J-lines for a dozen of galaxies, and found different excitation for the gas. When the gas mass could be derived from the dust emission however, the resulting values supported our adoption of the $\alpha = 0.8$ conversion factor (Combes *et al.* 2012). Mapping of some galaxies with the IRAM interferometer showed that the molecular gas is extended at kpc scales, and not only confined to a nuclear component (Combes *et al.* 2006, and in prep.).

Figure 1 shows that the data gap at intermediate redshift is now filled. The CO luminosities of starburst galaxies display an envelope which is constantly rising with redshift in this interval. The FIR to CO correlation is non-linear, and define gas depletion time between 6 and 600 Myr (Fig 1 right).

The gas fraction requires the determination of stellar mass, which was obtained through SED-fitting of optical and near-infrared luminosities (Combes *et al.* 2012). We define the

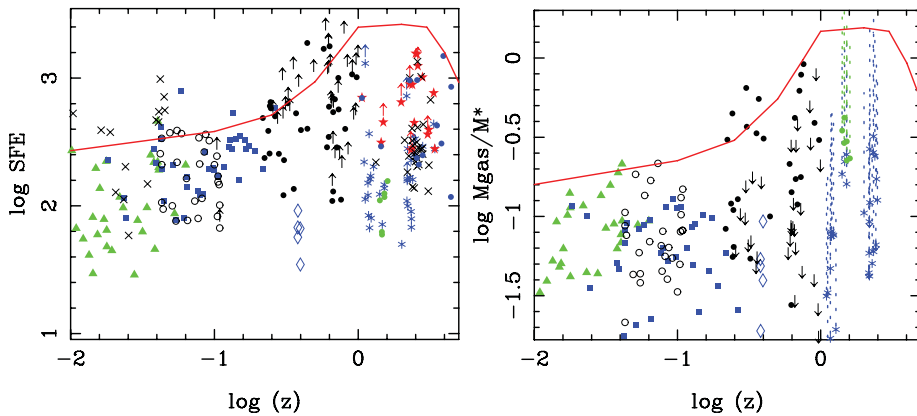


Figure 2. Left: The star formation efficiency versus redshift z . The symbols are the same as in Fig 1. The red curve is a schematic line summarizing the evolution of cosmic star formation density, from the compilation by Hopkins & Beacom (2006), complemented with recent work by Kistler *et al.* (2009) and Bouwens *et al.* (2008). This indicative curve is logarithmic and can be translated vertically. **Right:** The gas to stellar mass ratio vs redshift, with the same data. The points of the high- z samples (blue asterisks and green dots), have been continued by a dotted line joining the two extreme values of gas fraction, obtained with conversion factors $\alpha = 0.8$ and $4.6 M_{\odot} (\text{K km s}^{-1} \text{ pc}^2)^{-1}$.

star formation efficiency as the ratio of far infrared luminosity (proxy of star formation rate) and the molecular mass derived from the CO luminosity, with a constant conversion factor $\alpha = 0.8 M_{\odot} (\text{K km s}^{-1} \text{ pc}^2)^{-1}$. The SFE and gas fraction are plotted versus redshift and compared to available data in Fig 2. Both display an envelope which rises with redshift in the intermediate range between 0.2 and 1.0, the range where the cosmic star formation rate density is remarkably increasing by an order of magnitude. These trends are also visible in the bin-averages of the data, taking or not the upper limits into account (cf Fig 3).

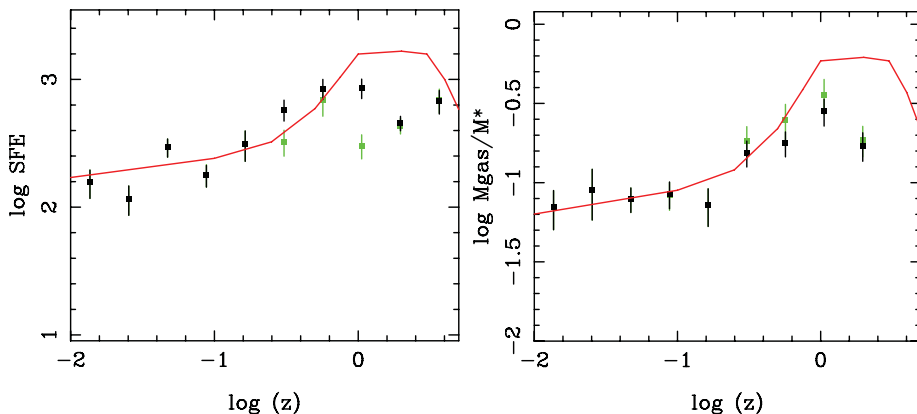


Figure 3. Evolution with redshift of averaged quantities, SFE at **left**, and gas to stellar mass ratio at **right**. The average of detected points only is plotted in green, and with the 3σ upper limits in black (for high- z samples only). The error bars are based on Poisson noise. The red line is the same as in Figure 2.

3. Conclusion

The increase of both star formation efficiency and gas fraction with redshift in the intermediate range for starburst galaxies suggests that both factors play a role in driving the evolution of the cosmic star formation rate density. The relative influence of each physical quantity is strongly linked to the CO-to-H₂ conversion factor. If a standard Milky Way ratio is used for these galaxies, their gas fraction will then dominate the evolution. We have tried to relate the star formation efficiency to the compactness of the starburst, measured from the half-light radius in the I-band (corresponding to the blue band in the rest frame). There is indeed an anticorrelation of SFE with half-light radius, but with a large scatter. The SFE was also plotted with respect to the specific star formation rate (or SFR per unit stellar mass), and compared to the locus of local “normal” star forming galaxies from the COLD GASS survey (Saintonge *et al.* 2011b). The starburst galaxies are globally located below, meaning that their gas content is significantly higher.

References

- Bouwens R. J., Illingworth G. D., Franx M., & Ford H. 2008, *ApJ* 686, 230
Chung, A., Narayanan, G., Yun, M. S., Heyer, M., & Erickson, N. R. 2009, *AJ* 138, 858
Combes, F., García-Burillo, S., Braine, J. *et al.* 2006, *A&A* 460, L49
Combes, F., García-Burillo, S., Braine, J. *et al.* 2011, *A&A* 528, A124
Conselice, C. J., Yang, C., & Bluck, A. F. L. 2009, *MNRAS* 394, 1956
Daddi E., Bournaud, F., Walter, F. *et al.* 2010 *ApJ* 713, 686
Gao Y. & Solomon P. M. 2004 *ApJS* 152, 63
Geach, J. E., Smail I., Coppin K. *et al.* 2009, *MNRAS* 395, L62
Geach, J. E., Smail I., Moran S. M. *et al.* 2011, *ApJ* 730, L19
Genzel, R., Tacconi, L. J., Gracia-Carpio, J. *et al.* 2010, *MNRAS* 407, 2091
Greve. T. R., Bertoldi, F., Smail, I. *et al.* 2005, *MNRAS* 359, 1165
Hopkins, A. M. & Beacom J. F. 2006, *ApJ*, 651, 142
Iono, D., Wilson, C. D., Yun, M. S. *et al.* 2009, *ApJ*, 695, 1537
Kartaltepe, J. S., Sanders, D. B., Le Floc'h, E. *et al.* 2010, *ApJ* 721, 98
Kistler M. D., Yüksel H., Beacom J. F. *et al.* 2009, *ApJ* 705, L104
Leroy, A. K., Walter, F., Brinks, E. *et al.* 2008, *AJ* 136, 2782
Madau P., Pozzetti L., & Dickinson M. E. 1998, *ApJ* 498, 106
Obreschkow, D., & Rawlings, S. 2009 *ApJ* 696, L129
Saintonge, A., Kauffmann, G., Kramer, C. *et al.* 2011a, *MNRAS* 415, 32
Saintonge, A., Kauffmann, G., Wang J. *et al.* 2011b, *MNRAS* 415, 61
Solomon P., Downes D., Radford S., & Barrett J. 1997, *ApJ* 478, 144
Solomon P. & Vanden Bout P. A. 2005, *ARAA* 43, 677
Tacconi L. J., Genzel R., Neri R. *et al.* 2010, *Nature* 463, 781